Cellulose (2024) 31:5575–5589
https://doi.org/10.1007/s10570-024-05942-5

ORIGINAL RESEARCH

# Characterization and value-added applications of natural cellulose fibers derived from cow dung in cementitious composites

**Zhengxian Yang · Kang Li · Xueyuan Yan · Wenda Wu · Bruno Briseghella · Giuseppe Carlo Marano**

Received: 11 November 2023 / Accepted: 1 May 2024 / Published online: 6 May 2024


**Abstract** Cow dung possesses potential agricultural and energy value but is often regarded as waste and underutilized in most cases. This wastage of resources not only poses a challenge to agricultural sustainability but also limits economic development in rural areas. Cow dung contains natural cellulose components like cellulose and lignin that are derived and used to prepare fiber materials. This paper explores a potential value-added application of agricultural waste, i.e., cow dung fibers to reinforce the alkali-activated slag composites (AASC), which are fabricated based on an industrial by-product slag. The raw and alkali treated cow dung fibers were characterized using scanning electron microscopy-energy dispersive X-ray spectroscopy (SEM–EDS), atomic force microscopy (AFM), X-ray photoelectron spectroscopy (XPS), thermo-gravimetric analysis (TGA) and X-ray diffraction (XRD). The porosity, density, water absorption, strength and drying shrinkage of AASC were tested and used to evaluate the effect of alkali treated fibers on the properties of AASC. The results showed that subjecting cow dung fibers to alkali treatment improved their surface roughness and thermal stability. The addition of cow dung fibers led to an augmentation in the splitting tensile strength of AASC, primarily due to the bridging action of these fibers. In particular, the 28-day splitting tensile strength of AASC containing 1 wt% of untreated cow dung fibers increased by 17.1% over the reference sample, and this increase was more pronounced in the alkali treated fiber sample. Moreover, the alkali treatment effectively reduced the effects of loss of compressive strength and increased drying shrinkage caused by fiber incorporation. The findings of this paper are helpful to solve the management problems of cow dung waste, reduce the environmental burden and realize the value utilization of resources.

**Keywords** Cow dung fibers · Alkali-activated slag composites · Treatment · Strength · Microstructure

**Supplementary Information** The online version contains supplementary material available at https://doi.org/10.1007/s10570-024-05942-5.

Z. Yang · K. Li · X. Yan · W. Wu · B. Briseghella
Joint International Research Laboratory of Deterioration and Control of Coastal and Marine Infra-Structures and Materials, College of Civil Engineering, Fuzhou University, Fuzhou 350108, China

W. Wu (✉)
College of Civil Engineering, Fuzhou University, Fuzhou 350116, China
e-mail: wenda@fzu.edu.cn; 281947484@qq.com

G. C. Marano
Department of Structural, Geotechnical and Building Engineering, Politecnico Di Torino, Corso Duca Degli Abruzzi, 24-10129 Turin, Italy

## Introduction

Alkali-activated slag (AAS) binder is considered to be a promising substitute for Portland cement and

has attracted wide attention in the field of civil engineering (Juenger et al. 2011; Elzeadani et al. 2022). Typically, it is prepared through a chemical reaction between an alkaline metal solution and slag at room temperature or slightly higher (Jiang et al. 2022). The resulting AAS cement is regarded as an eco-friendly construction material characterized by low energy consumption, excellent workability, superior strength, and exceptional durability (Mendes et al. 2021; Zhang et al. 2017). However, the application of AAS cement in building industry is still limited because of their inherently low tensile strength and large shrinkage, which can easily cause macroscopic or microscopic cracking and seriously affect their long-term durability (Zhang et al. 2022). To overcome the aforementioned issues, various fibers were commonly used to reinforce AAS-based cementitious composites. Yurt (2020) claimed that the addition of glass fibers has a beneficial impact on the splitting tensile strength of alkali-activated slag composites (AASC). Similarly, in a related research context, Zhou et al. (2021) pointed out that the flexural and splitting tensile strength of AAS concrete improved with higher basalt fiber content. However, concerns such as the high prices, poor biodegradation, and high energy consumption during production still need to be addressed for big-scale application of these fibers (Suwan et al. 2022). In this context, the exploration of alternative fibers becomes imperative to promote the sustainable development of construction materials.

Recently, natural fibers have shown great potential application in cementitious composites due to their cost-effectiveness, abundant availability, and eco-friendly nature (Santana et al. 2021; Li et al. 2022). Besides, the cementitious composites produced using natural fibers are relatively lightweight (Li et al. 2021). Despite many advantages the natural fibers having in enhancing alkali-activated materials, they still face the challenges of high water absorption and poor interfacial compatibility (Wei and Meyer 2015). The poor compatibility between natural fibers and the matrix is primarily attributed to the localized high moisture content at the interface zone between them. This heightened moisture content within natural fibers is a result of water absorption within their internal lumens. Therefore, we hypothesize that improving the interface compatibility between natural fibers and the matrix could be achieved by altering the lumen structure of natural fibers to prevent water absorption. One of the promising solutions to address these issues is appropriate surface treatment, which could increase the interfacial adherence of fibers to the matrix. Various treatment techniques have been proposed, such as alkali treatment (Bahja et al. 2021), silane treatment (Sepe et al. 2018), acetylation treatment (Joffre et al. 2017) and hornification treatment (do Amaral et al. 2022). Among these, alkali treatment stands out as the most prevalent and efficacious technique. This method involves immersing fibers in an alkaline solution, typically sodium hydroxide, for a period to eliminate the amorphous hemicellulose and lignin coatings on the fiber surface (Li et al. 2022). Moreover, alkali treatment has the capacity to induce the formation of a rough textures surface on the fibers, strengthening the mechanical interlocking between the fiber and the matrix (Vinod et al. 2021). According to Bootaphi et al. (2012), a 5% NaOH treatment was found to eliminate impurities from the surface of Borassus fruit fibers, enhancing their tensile properties and promoting improved interfacial properties within the composite. Huang et al. (2021) found by SEM analysis that alkali treated straw bond to AAS substrates to a higher degree than untreated straw. As reported by Andiç-Çakir et al. (2014), the treatment of coir fibers with 5% NaOH for duration of 2 h exhibited a significant improvement in the flexural strength and toughness of cementitious mortar.

Cow dung fiber is a natural lignocellulose fiber obtained by washing and separating cow dung. Cow dung is considered to be the residue of undigested food excreted by herbivores (cattle) and is an agricultural waste. Failing to promptly manage cow dung waste not only consumes substantial land but also results in environmental and atmospheric pollution in the vicinity. In recent decades, researchers have explored treatment options for cow dung waste (Reddy et al. 2013; Zhang and Sun 2017; Sfez et al. 2017). The most common method involves using it as a fuel source, but this approach releases a certain amount of greenhouse gases. Therefore, there is an urgent need to convert this discarded cow dung into resources with a high ecological value. In recent years, cow dung fibers have been found application in fabricating bio-composites with particular functionalities (Yusefi et al. 2018; Ma et al. 2019), providing a new thought for utilization of cow dung waste. Nonetheless, limited exploration has been carried out regarding the utilization of cow dung fibers in cementitious composites, especially in their role as an alternative reinforcement when creating AASC. Therefore, the primary objective of this work was to prepare a

sustainable AASC using industrial by-product slag and cow dung fibers. Scanning electron microscopy-energy dispersive X-ray spectroscopy (SEM–EDS), atomic force microscopy (AFM), X-ray photoelectron spectroscopy (XPS), thermo-gravimetric analysis (TGA) and X-ray diffraction (XRD) were applied to clarify the effect of alkali treatment on the morphology and physicochemical behavior of cow dung fibers. The influence of alkali treated cow dung fibers on the properties of AASC was investigated by testing the porosity, density, water absorption, strength and drying shrinkage of AASC. The hydration characteristics of AASC were assessed by hydration heat, TGA, XRD, Fourier transform infrared spectrometry (FTIR) and SEM–EDS.

## Experimental section

### Materials

The ground granulated blast-furnace slag (GGBS) used in this study is the comminuted product of rapidly quenched blast-furnace slag separated from molten pig iron and provided by Longze Water Purification Materials Company in Gongyi, China. Table 1 shows the chemical composition of GGBS. The alkali activator was made by dissolving NaOH flakes in deionized water. NaOH (purity higher than 96%) was supplied by Sinopharm Chemical Reagent Company, China. The specific gravity of the standard sand is 2.63 g/cm$^3$ and the fineness modulus is 2.48. In addition, the PS utilized to adjust the workability of fresh AASC was purchased from Zhongyan Technology Company in Hunan, China. The cow dung fibers were received from a farm at Henan Agricultural University, China. A typical extraction and separation process for producing the cow dung fiber is shown in Fig. 1a. The physical properties and chemical composition of cow dung fibers are given in Tables 2 and 3 respectively. Notably, cow dung fibers exhibit a substantial cellulose content, a crucial reinforcing component within cementitious composites. Consequently, the efficient repurposing of cow dung waste for employment in cementitious composite fabrication aligns with the principles of sustainable development.

**Table 1** Chemical composition of GGBS

| $Al_2O_3$ | CaO | $SiO_2$ | MgO | $SO_3$ | $Fe_2O_3$ | $Na_2O$ | $TiO_2$ | Other | LoI |
|---|---|---|---|---|---|---|---|---|---|
| 13.00 | 47.00 | 21.90 | 8.07 | 2.50 | 0.74 | 0.33 | 0.89 | 2.93 | 2.28 |

*LOI* loss on ignition

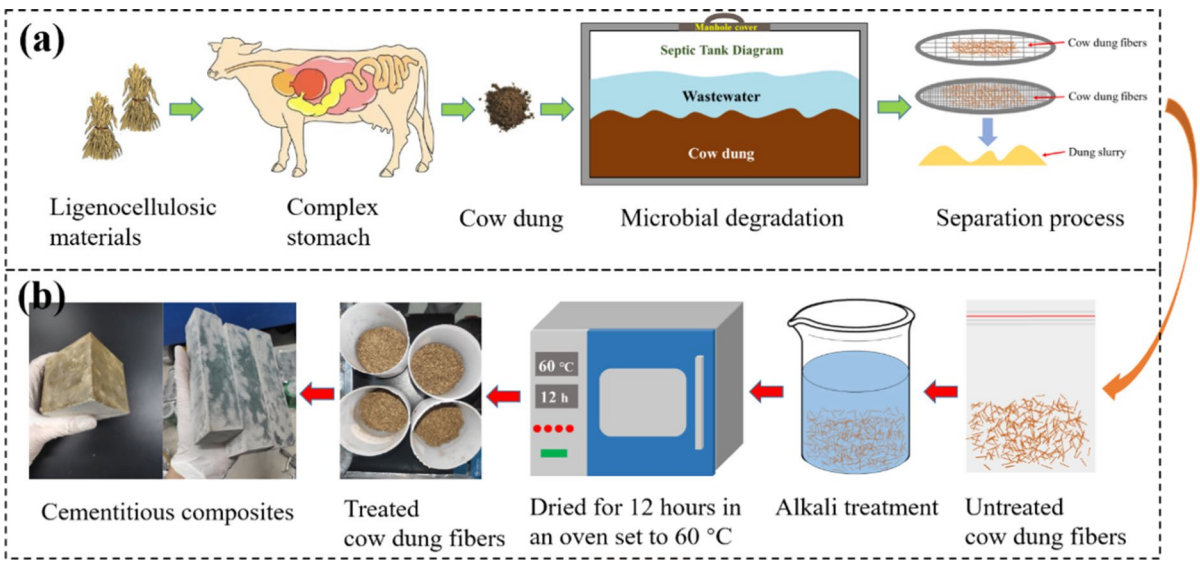


**Fig. 1** Flow chart of (**a**) extraction and separation and (**b**) alkali treatment of cow dung fibers

**Table 2** Physical properties of cow dung fibers

| Properties | Density ($g/cm^3$) | Length (μm) | Average diameter (μm) | Aspect ratio |
|---|---|---|---|---|
| Cow dung fiber | 1.37 | 10000 | 220.54 | 45.34 |

**Table 3** Chemical composition of cow dung fiber Reproduced from Yang et al. (2023)

| Holocellulose | Cellulose | Lignin | Ash |
|---|---|---|---|
| 69.86 | 47.00 | 21.90 | 8.07 |

### Alkali treatment of cow dung fibers

The alkali treatment of cow dung fibers was performed by soaking the fibers in a 1 M NaOH solution for 12 h. Then, the cow dung fibers were washed 3–4 times with deionized water to remove the residual alkali. These fibers were then placed in a drying oven and dried at a constant temperature of 60 ℃ for 12 h to remove moisture before collecting in sealed bags for subsequent experiments. Figure 1b shows the process of alkali treatment.

### Preparation of AASC with cow dung fibers

Nine mix proportions were used in this experiment to investigate the effects of cow dung fibers on the properties of AASC. The cow dung fiber content ranged from 0 to 2% of the overall binder mass, with the binder mass being the combined mass of NaOH and GGBS. For each mixture, the ratio of water to binder is fixed at 0.5. The mass ratio of sand to binder is kept at 3:1. The reference mix without cow dung fibers was prepared for comparison purposes. The details of all mix are given in Table 4. The ID of each mixture is divided into two parts: the first part represents fiber type (untreated or treated) and the second part indicates the fiber content (0–2% by binder mass). For example, the mixture UF0.5 means that the content of untreated cow dung fibers is 0.5%.

To prevent the agglomeration between the fibers, a pre-mixing step was performed with the cow dung fibers and the NaOH solution at a concentration of 2.3 M, followed by subjecting the mixture to 30 min of ultrasonic treatment using the KQ-250 ultrasonic generator. The ultrasonic frequency and power was 40 kHz and 250 W respectively. Subsequently, GGBS and sand were incrementally introduced into a mixer for a dry blending duration of 2 min. Finally, the fiber-activator blend from the ultrasonic step was gently poured into the mixer and stirred at low speed for 2 min, followed by 2 min of high-speed stirring. The preparation procedure of AASC is depicted in Fig. S1. It has to be point out that the activator should have enough time to cool down before casting as it releases heat during preparation. Once the mixing process is complete, the mixture is poured into a mold, subjected to one minute of vibration using a shaker to eliminate trapped bubbles, and then sealed with a film to maintain moisture. Following this, the specimens are allowed to cure at the laboratory's ambient temperature for 24 h and are later transferred to a curing room set at 98% relative

**Table 4** Mix proportion of AASC

| Samples | Mix ID | Cow dung fiber | | GGBS (g) | NaOH (g) | Sand (g) | Water (g) | PS (g) |
|---|---|---|---|---|---|---|---|---|
| | | Content (%Binder) | Type | | | | | |
| Ref. | Ref. | 0 | - | 428.6 | 21.4 | 1350 | 225 | 0.675 |
| UF-AASC | UF0.5 | 0.5 | Untreated | 428.6 | 21.4 | 1350 | 225 | 0.675 |
| | UF1.0 | 1.0 | Untreated | 428.6 | 21.4 | 1350 | 225 | 0.675 |
| | UF1.5 | 1.5 | Untreated | 428.6 | 21.4 | 1350 | 225 | 0.675 |
| | UF2.0 | 2.0 | Untreated | 428.6 | 21.4 | 1350 | 225 | 0.675 |
| TF-AASC | TF0.5 | 0.5 | Treated | 428.6 | 21.4 | 1350 | 225 | 0.675 |
| | TF1.0 | 1.0 | Treated | 428.6 | 21.4 | 1350 | 225 | 0.675 |
| | TF1.5 | 1.5 | Treated | 428.6 | 21.4 | 1350 | 225 | 0.675 |
| | TF2.0 | 2.0 | Treated | 428.6 | 21.4 | 1350 | 225 | 0.675 |

humidity and 20 ℃, where they remain until reaching the specified age.

## Testing methods

### *Characteristics of cow dung fibers*

The surface morphology and elemental composition of cow dung fibers were conducted by SEM–EDS. The fiber specimens are adhered to the tape and then gold plated on their surfaces to improve conductivity. The Quanta 250 provided by FEI was used in this experiment and operated at a voltage of 30 kV. Optical microscopes were also used to observe the surface of cow dung fibers. The surface roughness of cow dung fibers was assessed using AFM (AFM-5500, Agilent, USA) with a scanning area of 2 μm × 2 μm. For the characterization of XPS C1s spectra of fibers, an XPS instrument (ESCALAB 250 Xi, Thermo, USA) was employed, featuring a 500 μm spot size and 20 eV pass energy. TGA of cow dung fibers were carried out by a thermal analyzer (STA449 F5, Netzsch, Germany) with a heating rate of 10 °C/min from room temperature to 600 °C. The amorphous and crystalline peaks of the cow dung fibers were determined using X-ray diffraction (X'pert3, Panalytical, Netherlands). The scanning range was from 5° to 60° 2θ at 40 kV and 40 mA.

### *Porosity, bulk density and water absorption*

Referring to ASTM C642, the cubic samples with a size of 70 mm × 70 mm × 70 mm were used for testing porosity, bulk density and water absorption of AASC. Three samples were determined for each mixture. The following equations were used to calculate porosity, bulk density and water absorption.

$$\text{porosity} = \frac{m_2 - m_0}{m_2 - m_3} \times 100\% \quad (1)$$

$$\text{bulk density (g/cm}^3\text{)} = \frac{m_0}{m_2 - m_3} \quad (2)$$

$$\text{water} = \frac{m_1 - m_0}{m_0} \times 100\% \quad (3)$$

where $m_0$ is the mass of the sample after drying, $m_1$ is the mass of the sample after immersion, $m_2$ is the mass of the sample in air after immersion and boiling, and $m_3$ is the mass of the sample in water after immersion and boiling.

## Mechanical properties

According to ASTM C39/C39M and ASTM C496/C496M, cylindrical specimens measuring 50 mm in diameter and 100 mm in height were employed to measure the compressive and splitting tensile strength at 3, 14 and 28 days of standard curing. Each set of measurements was based on three samples, and the results were averaged.

## Drying shrinkage

The drying shrinkage of AASC was measured based on ASTM C596. Specimens with dimensions of 25 mm × 25 mm × 280 mm were prepared and demoulded after 24 h. Then, the specimens were stored in a curing room with 45 ± 4% RH at 20 ± 2 °C. A comparator was used to determine the length change of the specimens regularly until 35 days. Three replicates were tested for each mixture.

## Hydration characteristic

The hydration characteristics of AASC were evaluated using heat of hydration, TGA, XRD and FTIR. The hydration heat of AASC was determined by a TAM air isothermal calorimeter over a 24-h period. Mixing of each paste was completed in an insulated sealed bag. Ten grams of fresh paste was quickly injected into the ampoule using a syringe, sealed and placed in the channel of the calorimeter. To reduce the noise signal ratio, ampoules containing deionized water are placed in the adjacent channels for reference. The TGA of AASC was carried out in the range of room temperature to 1000 °C, and the other test conditions were the same as Section 2.4.1. The hydration products of AASC were analyzed by XRD (X'Pert3, Panalytical, Netherlands, 2θ range of 5–60° at 40 kV and 40 mA) and FTIR (Nicolet iS50 spectrometer, Thermo Scientific, USA, spectral range of 4000–500 $cm^{-1}$ at the resolution of 2 $cm^{-1}$.

Morphological analysis

The microstructure and phase of AASC were observed by SEM–EDS (Quanta 250, FEI, USA). The specimens used for the test were broken cylindrical mortar specimens cut into 10 mm × 10 mm sizes, then cleaned and dried. The accelerating voltage was 15 kV, and all samples were coated with a layer of gold to increase the conductivity before observation.

## Results and discussion

Characteristics of cow dung fibers

The appearance images of untreated and treated cow dung fibers are shown in Fig. 2a and e, respectively. The diameter of the treated fibers significantly decreased, attributed to the removal of amorphous components during the treatment process. In addition, this treatment breaks down fiber bundles into finer fibers, thereby increasing their effective surface area (Van Nguyen and Mangat 2020). Figure 2b and f illustrate the surface morphology of untreated and treated cow dung fibers. From Fig. 2b, it can be observed that impurities were present on the fiber surface. Conversely, as depicted in Fig. 2f, the treated cow dung fibers displayed a markedly cleaner and rougher surface texture. Actually, the rough surface of treated cow dung fibers was attributed to some hemicellulose, lignin and pectin dissolved in an alkaline solution. As can be seen in Fig. 2c, an abundance of lumens was evident within untreated cow dung fibers. Nevertheless, following the application of an alkali treatment, as depicted in Fig. 2g, the lumens in cow dung fibers became imperceptible. Shang et al. (2020) documented that the alkali treatment-induced contraction or closure of these lumens in straw fibers led to a decrease in their water absorption capacity, potentially mitigating any detrimental effects on the cement matrix. The corresponding EDS results are illustrated in Fig. 2d and h. It can be observed that untreated cow dung fibers show a significant presence of elemental carbon (C) and oxygen (O), which is due to the organic phase of cellulose. However, the reduced content of elemental C after treatment suggests that the treatment induces the precipitation of certain carbon-containing substances from the fibers. It is noteworthy that the increased content of Na elements is the result of alkaline substances remaining on the fiber surface. Figure S2 presents the 3DAFM images of untreated and treated cow dung fibers. In Fig. S2a, it is evident that the untreated cow dung fibers exhibit a Root-mean-square (RMS) roughness of 1.78 nm. The RMS roughness of the treated cow dung fibers was 7.76 nm (Fig. S2b). The alkali treatment caused the fiber surface to show more pronounced grooves and increased the roughness, as is additionally verified in the SEM images (Fig. 2b and f). Obviously, heightened roughness promotes enhanced interlocking between the fibers and the matrix, consequently leading to an improved interfacial bond between them.

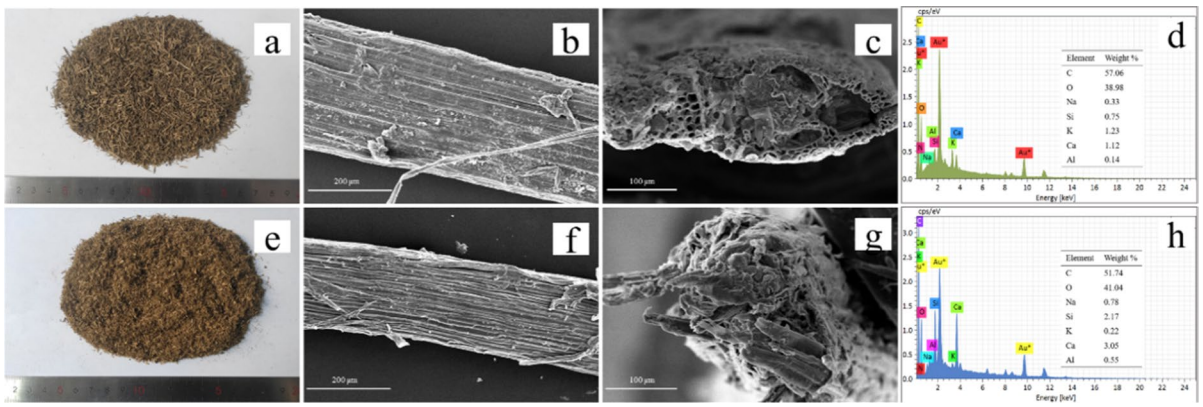


**Fig. 2** Images of cow dung fibers (**a**) appearance of untreated fibers (**b**) SEM images of untreated fiber surface (**c**) SEM images of untreated fiber cross-section (**d**) EDS analyses of untreated fibers (**e**) appearance of treated fibers (**f**) SEM images of treated fiber surface (**g**) SEM images of treated fiber cross-section (**h**) EDS analyses of treated fibers

Figure 3a shows the XPS wide scans spectra of untreated and treated cow dung fibers. It can be seen that O and C are the major elements on the surface of cow dung fibers. In addition, the treated cow dung fibers exhibit a new peak around 1071 eV, indicative of the presence of Na element, a result of the surface modification caused by the NaOH solution. The XPS C1s spectra of untreated and treated cow dung fibers are shown in Fig. 3b and c. Typically, carbon in cow dung fiber exists in three binding forms: C1 (C–C/C-H), C2 (C-O), and C3 (C=O/O-C-O). The ratio of C1 to C2 values is indicative of the lignin content in natural cellulose fibers (Tang et al. 2023). As indicated in Table 5, the C1/C2 value for the treated fibers (2.13) surpassed that of the untreated (1.79), signifying the effective removal of lignin through alkali treatment. These findings align with the SEM–EDS results in Fig. 2.

The TG-DTG analysis for untreated and treated cow dung fibers is given in Fig. 3d and e. The decrease in fiber weight can be categorized into three phases. The initial phase occurs between 35 and 105 °C, and this can be ascribed to the desiccation of moisture within the fiber. The second phase of mass loss appears at 150–238 °C and is result of the decomposition of the amorphous components. The last phase of degradation takes place within the range of 258 to 360 °C, which corresponds to the decomposition of α-cellulose. The highest decomposition temperature can serve as an indicator of the raw material's thermal stability. The DTG curve shows that the maximum decomposition temperatures of untreated and treated cow dung fibers are 335 °C and 347 °C, respectively, signifying an enhancement in thermal stability resulting from the treatment. Additionally, the weight loss ratio of alkali

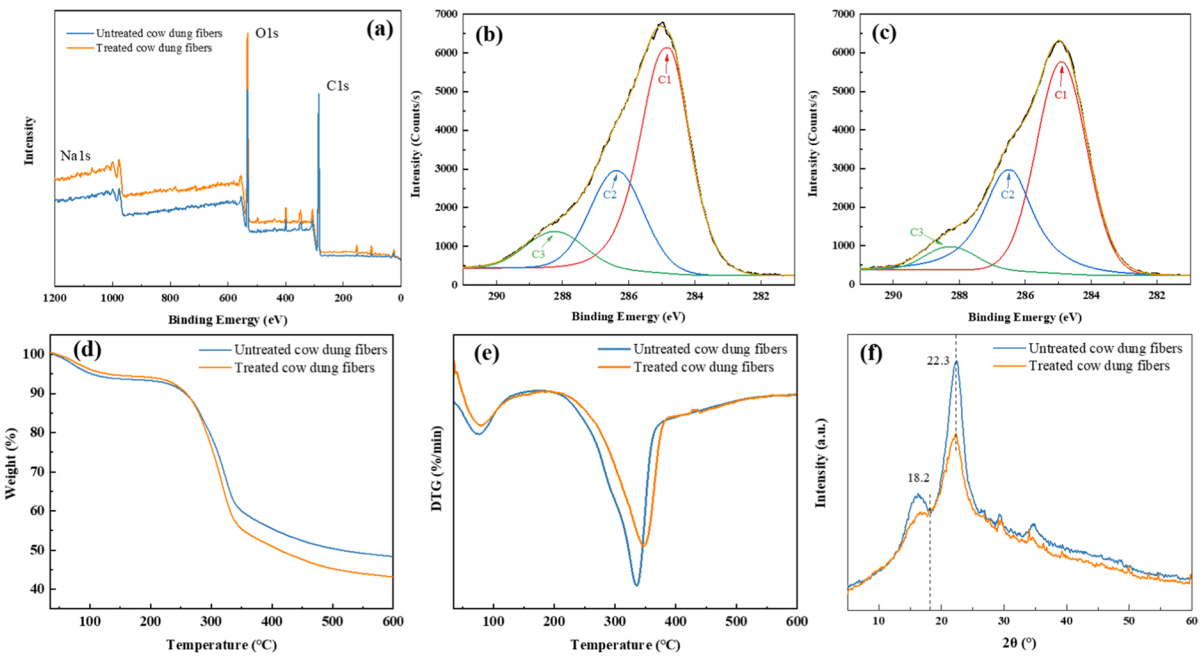


**Fig. 3** XPS wide scans spectra of untreated and treated cow dung and fibers (**a**). XPS C1s spectra of untreated and treated cow dung fibers (**b, c**). TG-DTG curves of untreated and treated cow dung fibers (**d, e**). XRD patterns of untreated and treated cow dung fibers (**f**)

**Table 5** XPS results of untreated and treated cow dung fibers

| Cow dung fibers | Peak area | | | Relative content (%) | | | C1/C2 |
|---|---|---|---|---|---|---|---|
| | C1 | C2 | C3 | C1 | C2 | C3 | |
| Untreated | 57,784.49 | 27,084.11 | 10,775.13 | 60.40 | 28.32 | 11.28 | 2.13 |
| Treated | 52,761.63 | 29,515.64 | 5776.99 | 59.91 | 33.53 | 6.56 | 1.79 |

treated cow dung fibers (57.1%) between 35–600 °C is higher than that of untreated cow dung fibers (51.6%), due to the removal of amorphous components during alkali treatment. These findings align with the conclusions documented in prior studies by Li et al. (2022) and Vinod et al. (2021).

Figure 3f shows the XRD results for untreated and treated cow dung fibers. The maximum peak representing crystalline macromolecules appeared at 2θ = 22.3° and the minimum peak representing amorphous macromolecules appeared at 2θ = 18.2° for both test samples. Based on the results in Fig. 3f, the empirical Eq. (4) proposed by Segal et al. (1959) was used to calculate the crystallinity index (CI) of cellulose, with the results presented in Table 6. The crystallinity index of alkali treated cow dung fibers increased from 45.2% for the untreated cow dung fibers to 60.2%. A similar observation has been made for hemp and Alfa fibers when treated with alkali (Le Troëdec et al. 2008; Borchani et al. 2015). Alkali treatment removes the amorphous parts of the plant and after treatment the material contains more crystalline cellulose regions as a result the degree of crystallinity increases (Le Troëdec et al. 2008; Borchani et al. 2015).

$$CI = \frac{I_{200} - I_{am}}{I_{200}} \times 100 \quad (4)$$

where $I_{200}$ represents the maximum intensity of diffraction of the (200) lattice peak at 2θ: 22°-23°, and $I_{am}$ represents the intensity of diffraction of the amorphous part which is taken at 2θ: 18°-19°.

## Porosity, bulk density and water absorption of AASC

As depicted in Fig. 4a, the introduction of cow dung fibers in AASC results in an elevated porosity. Importantly, the porosity increase for TF-AASC is more gradual than that observed in UF-AASC.

**Table 6** Crystallinity index of untreated and treated cow dung fibers

| Cow dung fibers | Untreated | Treated |
|---|---|---|
| $I_{am}$ | 670 | 668 |
| $I_{200}$ | 1223 | 1678 |
| Crystallinity index (%) | 45.2% | 60.2% |

In comparison to the reference sample's porosity, UF2.0 and TF2.0 exhibited increases of 14.97% and 6.88%, respectively, suggesting that alkali treatment has the potential to mitigate the entrainment of air by cow dung fibers. The results depicting the variation in bulk density of AASC in relation fiber content are shown in Fig. 4b. The bulk density of all AASC fell within a range of 2.01 g/cm$^3$ (without cow dung fibers) and 1.92 g/cm$^3$ (2% untreated cow dung fibers), and consistently decreased as the fiber content increased. These findings align with previous studies conducted by Alomayri et al. (2013) and Poletanovic et al. (2020). Alomayri et al. noted a decrease in the bulk density of alkali-activated fly ash composites with increasing cotton fiber content. Similarly, Poletanovic et al. found that incorporating hemp fibers led to a reduction in the bulk density of AAS mortar. It is of interest that the bulk density of AASC with treated cow dung fibers surpasses that of AASC with untreated cow dung fibers. This occurs because the inclusion of treated cow dung fibers increases the compactness of AASC, thereby reducing its porosity in the hardened state, resulting in an increase in bulk density. From Fig. 4c, it can be observed that the water absorption of AASC increases with the increase in content of cow dung fiber content and this phenomenon is attributed to the increase in matrix porosity. Furthermore, when an equivalent amount of fibers was used, the water absorption of AASC reinforced with treated cow dung fibers proved to be less than that of specimens incorporating untreated cow dung fibers. In the similar lines, Jiang et al. (2020) pointed out that straw fibers became smaller and finer after alkali treatment. These fine fibers become tightly bound to the matrix. With the decrease in porosity, the water absorption of cement-based composites decreases.

## Mechanical properties

The compressive strength of cow dung fiber reinforced AASC at 3, 14 and 28 days of curing is given in Fig. 5a and b. The results show that the incorporation of cow dung fibers leads to a decrease in strength at all curing ages compared to the Ref. Specifically, the maximum reduction at 3, 14 and 28 days are 40.8%, 56.4% and 53.4%, respectively, for UF2.0 samples as shown in Fig. 5a. However, it is notable that the AASC reinforced with treated

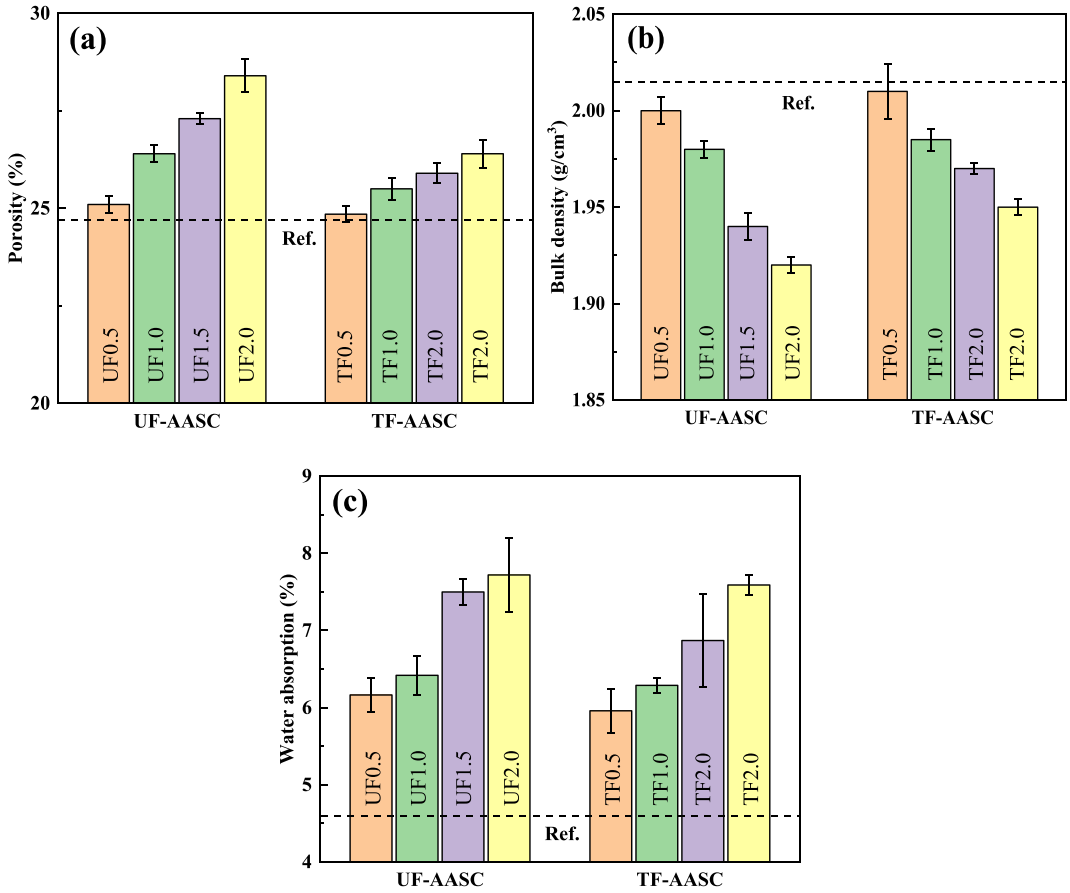


**Fig. 4** **a** Porosity, **b** bulk density and **c** water absorption of AASC

cow dung fibers exhibited greater strength compared to their untreated counterparts, as demonstrated in Fig. 5b. For example, compared with UF2.0 specimen, the compressive strength of the TF2.0 specimen improved by 32.6%, 52.4% and 51.7% at 3, 14 and 28 days, respectively. The increase in strength is considered to be a result of the improved adhesion between the treated cow dung fibers and the AASC matrix. Figure 5c and d illustrates the variation of splitting tensile strength of AASC with cow dung fiber content after curing for 3, 14 and 28 days. As seen in Fig. 5c and d, the splitting tensile strength of AASC increases and then decreases as the content of cow dung fibers increases, reaching a maximum at 1%. When the fiber content was 1% (UF1.0 sample), the splitting tensile strength of AASC at 3, 14 and 28 days increased by 27.5%, 18.5% and 17.1%, respectively, compared to the reference sample (Ref.). This behavior can be interpreted as the stress in the composite samples can be transferred to the fibers through the interface with the matrix (Wongsa et al. 2020). As the fiber content was further increased from 1 to 2%, the decrease in splitting tensile strength could be attributed to an excess of fiber bundles distributed parallel to the splitting surfaces resulting in more weak surfaces as well as insufficient contact between the slag particles. The higher the cow dung fiber content, the greater the risk of damage along these weak surfaces. Moreover, by comparing the results of Fig. 5c and d, it can be seen that both cow dung fibers significantly improved the splitting tensile strength of AASC, but the treated fibers showed a higher reinforcement effect. Particularly, compared with UF1.0 samples, the splitting tensile strength of TF1.0 samples at 3, 14 and 28 days increased by 14.4%, 17.8% and 17.6%, respectively. This occurs because the adhesion between the fiber surface and the matrix

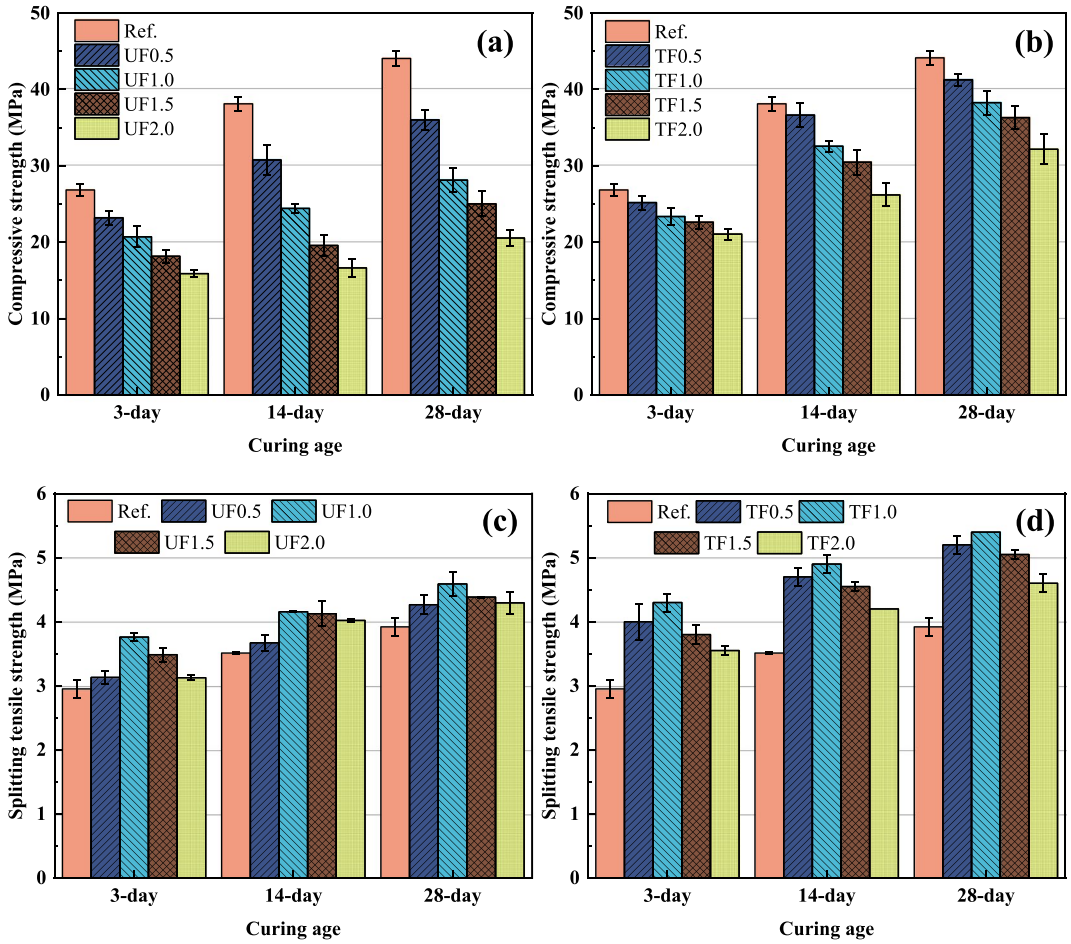


**Fig. 5** Compressive strength of AASC reinforced with untreated and treated cow dung fibers (**a**, **b**). Splitting tensile strength of AASC reinforced with untreated and treated cow dung fibers (**c**, **d**)

strengthens as it becomes rough. Consequently, this enhancement leads to an increase in the splitting tensile strength of AASC.

To reveal the main factor of strength reduction, Ryshkewitch's empirical formula was employed to fit the relationship between compressive strength and porosity. The results are depicted in Fig. S3, where the correlation coefficient ($R^2$) stands at 0.9223, demonstrating a strong correlation between compressive strength and porosity. The influence of the fiber-matrix interface on compressive strength appears to be constrained. The increase in fiber content reduces the density of AASC, making it challenging to pack the AASC matrix. As a result, the porosity of AASC increases, leading to a subsequent reduction in compressive strength. This finding is similar to the results obtained for sisal and coconut fiber reinforced alkali-activated fly ash composites (Wongsa et al. 2020).

$$\sigma = \sigma_0 e^{-kP} \tag{5}$$

where $\sigma$ = strength; $\sigma_0$ = strength at zero porosity; k = empirical constant; P = porosity.

## Drying shrinkage

Figure 6 shows the drying shrinkage of AASC. It is evident that the presence of cow dung fibers increased the drying shrinkage of AASC. The higher the fiber content, the more pronounced the drying shrinkage becomes. After 35 days of drying, the shrinkage in AASC reinforced with 1% and 2% cow dung fibers

exceeded that of the reference specimen by 19.7% and 33.8%, respectively. Generally, it is accepted that the drying shrinkage of concrete is primarily influenced by its porosity and the continuity of the capillary system within the hydrated paste (Toledo Filho et al. 2005). Adding cow dung fibers increased the porosity of the matrix and created cross-linked moisture migration channels, which caused the increase of drying shrinkage. This is confirmed by the results of the porosity and water absorption tests. It is notable that samples containing treated cow dung fibers exhibited lower drying shrinkage than samples containing untreated cow dung fibers. At 35 days, the drying shrinkage of TF0.5, TF1.0, TF1.5 and TF2.0 decreased by 3.8%, 7.9%, 8.9% and 10.1% compared with UF0.5, UF1.0, UF1.5 and UF2.0, respectively. A primary objective of alkali treatment is to remove amorphous impurities from the fibers, resulting in enhanced embedding of the fibers within the matrix, thereby dispersing and absorbing stresses caused by drying shrinkage more efficiently and reducing crack formation (Tong et al. 2014).

## Hydration of AASC

The heat flow and cumulative heat results of three AAS pastes are plotted in Fig. S4. The incorporation of cow dung fibers retarded the thermal evolution rate and the main peak of heat flow. The main peak values of heat flow were 5.254 and 7.118 mW/g for UF1.0 and TF1.0, respectively. Moreover, the time of the highest peak appeared in TF1.0 was advanced by 0.50 h in comparison with that of UF1.0. This is because the soluble substances in the untreated cow dung fibers complexed with $Ca^{2+}$ released during slag cement hydration and hindered the hydration of the slag cement (Guo et al. 2019). As can be seen from the cumulative heat curves that the hydration heat release of UF1.0 is lower than that of Ref. This may be because the cow dung fibers with strong water absorption ability absorbs the mixing water of the system when it is incorporated into the AAS matrix, resulting in a smaller contact area between the slag particles and the water, thereby limiting the release of hydration heat. However, the cumulative heat of TF1.0 exceeds that of UF1.0 as well as Ref., indicating that the alkali treatment effectively eliminates the negative effect of untreated cow dung fibers on the hydration of AAS cement.

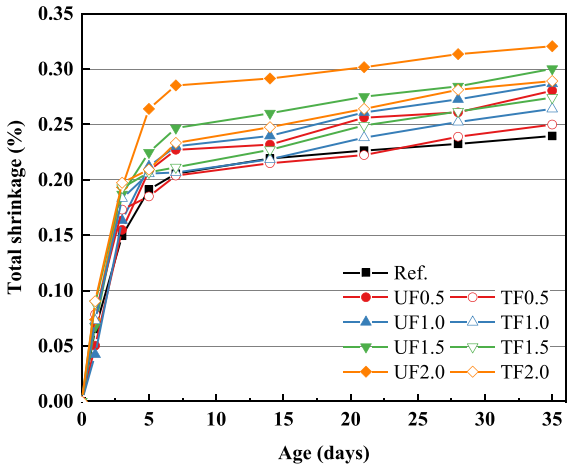


**Fig. 6** Drying shrinkage of AASC reinforced with untreated and treated cow dung fibers

TG and DTG curves of three AAS pastes are shown in Fig. S5. The mass loss in the range of 40–200 °C and 640–860 °C corresponded to the decomposition of C-(A)-S–H and $CaCO_3$, respectively (Tang et al. 2023). The mass loss in the range of room temperature to 1000 °C can reflect the degree of hydration of the sample, so the greater the weight loss in this range, the more the hydration products. The mass loss of Ref. (17.34%) at room temperature to 1000 °C was larger than that of UF1.0 (15.90%) and less than that of TF1.0 (18.81%). This indicates that the addition of untreated fibers hinders slag cement hydration while the addition of treated fibers promotes slag cement hydration (Shang et al. 2020). This explains well the findings of the heat of hydration test.

Figure S6 displays the XRD patterns of AAS pastes. The characteristic peaks at 2θ angles of 23.04°, 29.44°, 36.58°, 39.51°, 47.56° and 48.50° are indicative of calcite ($CaCO_3$, PDF # 01–081-2027), confirming carbonization in all three AAS pastes. The peak intensity of UF1.0 exceeded that of the reference sample (Ref.) but fell short of TF1.0, indicating that UF1.0 exhibited the highest degree of carbonization, followed by TF1.0, and then Ref. This variance is attributable to the porous structure of natural cow dung fibers, which facilitates the penetration of $CO_2$ and $H_2O$ into the AAS matrix (Huang et al. 2022). The carbonate solution's interaction with the calcium-rich calcium aluminate silicate hydrate (C-A-S–H) phase in AAS leads to

partial decalcification of C-A-S–H, resulting in the loss of AAS matrix cohesion and the formation of large pores (Huang et al. 2022), subsequently reducing the compressive strength of AAS. It is notable that alkali treatment reduces the porosity of the AAS matrix and the degree of carbonization by mitigating the entrainment air effect caused by cow dung fibers.

The changes of chemical groups in the reaction products were investigated using FTIR spectra and the results are shown in Fig. S7. The absorption peaks at 3420 $cm^{-1}$ and 1642 $cm^{-1}$ correspond to the stretching vibration of -OH and the bending vibrations of H–O-H, respectively, indicating the presence of crystallization water in the AAS paste (Si et al. 2023). The spectral bands at 1415 $cm^{-1}$ and 873 $cm^{-1}$ are associated with the asymmetric stretching vibration of $CO_3^{2-}$, characteristic of calcite, suggesting carbonation of the AAS gel (Sun et al. 2023). Peaks near 950 $cm^{-1}$ result from the asymmetric stretching vibration of Si–O-T (Si or Al) (Huang et al. 2022), with higher wavelengths in the Ref. sample (950 $cm^{-1}$) and UF1.0 sample (952 $cm^{-1}$) indicating decalcification of the calcium-sodium aluminosilicate hydrate (C-(N)-A-S–H) gels, detrimental to aluminosilicate gel formation (Zhou et al. 2020). This decalcification and depolymerization are also observed in AAS gels (Huang et al. 2022). XRD results confirm that AAS gels' decalcification and depolymerization are due to carbonation. While the TF1.0 sample, the lower wavelength (945 $cm^{-1}$) of Si–O-T (Si or Al) suggests the formation of more N-A-S–H or C-A-S–H gels. Therefore, the C-A-S–H gels in the TF1.0 samples were not seriously impaired by excessive carbonation, which suggests that the alkali treatment improved the durability of AASC.

### SEM–EDS analysis of AASC

Figure 7 illustrates the SEM–EDS results of AASC reinforced with untreated and treated cow dung fibers. As shown in Fig. 7a, the presence of a discernible interfacial transition zone between the fiber and the matrix, suggesting poor adhesion at the fiber-matrix interface. However, the treated cow dung fibers are tightly bound to the AASC matrix and covered by the hydration products, as shown in Fig. 7c. The improvement in the interface transition zone at the cow dung fiber-matrix after alkali treatment, along with SEM images showing the cross-section of cow dung fibers shown in Fig. 2c and g, supports our hypothesis that alkali treatment can enhance the interface compatibility between cow dung fibers and AASC matrix by shrinking or closing the lumens of cow dung fibers. EDS analysis of the AASC matrix (Fig. 7b and d) revealed that the weight percentage of elemental C at point 1 was 9.3%, and the C content at point 2 was reduced by 24.1% compared to point 1. This is related to the participation of C-containing substances precipitated from plant fibers in an alkaline environment are involved in the chemical reaction of AASC (Zhou et al. 2020). It is noted that the Si, Al and Ca elements in point 2 are significantly more than those in point 1, which are the main elements of cement hydration product calcium silicate hydrates (C-S–H), indicating that alkali treated cow dung fibers can promote cement hydration and thus produce more hydration products than untreated cow dung fibers. These observations align with the findings outlined in the section on heat of hydration. In addition, this is the reason why the strength of AASC with treated cow dung fibers is higher than that with untreated cow dung fibers (Fig. 5).

## Conclusions

In this paper, natural cellulose fibers were derived from cow dung waste as a reinforcement for AASC to achieve a value-added recycling of industrial by-products and agricultural wastes. The following conclusions were drawn:

- Alkali treatment partially removed amorphous hemicellulose and lignin in the cow dung fibers, which increased the surface roughness of the fibers and thus strengthened the fiber-matrix interfacial bonding.
- The addition of cow dung fibers effectively increased the splitting tensile strength of AASC through the "bridging action" between matrix and fibers. In addition, following a 28-day cur-

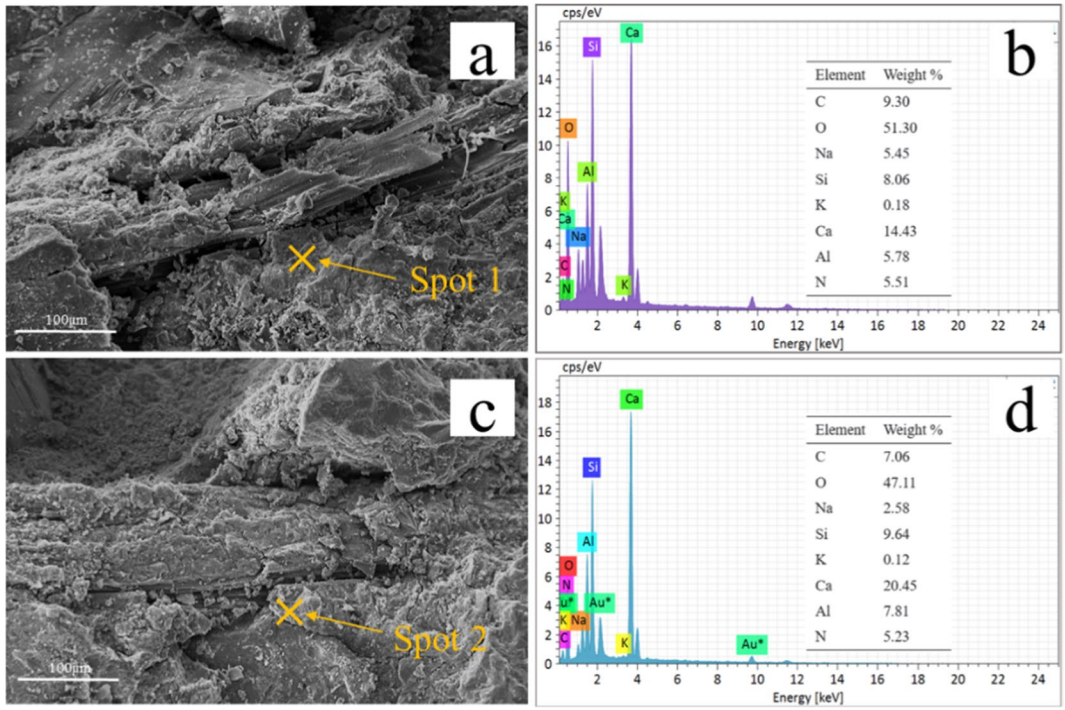


**Fig. 7** SEM images (**a**) AASC with untreated cow dung fibers (**b**) EDS analyses of spot 1 (**c**) AASC with treated cow dung fibers (**d**) EDS analyses of spot 2

ing period, the splitting tensile strength of TF1.0 increased by 17.6% compared to that of UF1.0.

- The compressive strength of AASC is closely associated with its porosity. The incorporation of cow dung fibers decreased the density and increased the porosity of AASC. However, the alkali treatment mitigated the air-entraining effect of cow dung fibers and decreased the porosity of the matrix, so that the loss of compressive strength of AASC caused by fiber incorporation was effectively mitigated.
- Alkali treatment ameliorated the negative effect of soluble substances in untreated cow dung fibers on slag cement hydration. In addition, more N-A-S–H or C-A-S–H gels were formed in TF1.0 compared to UF1.0, suggesting that the C-A-S–H gels in TF1.0 were not severely damaged by excessive carbonation, demonstrating that the alkali treatment improved the durability of AASC.
- SEM images reveal a distinct interface transition zone between untreated cow dung fibers and the matrix, indicating poor adhesion between the matrix and fibers. However, after alkali treatment, cow dung fibers are tightly bound to the matrix and covered by hydration products. In addition, hydration heat and EDS results suggest that alkali treatment promotes the hydration of AAS cement, resulting in more hydration products compared to untreated cow dung fibers.

In summary, cow dung fibers are a readily available and renewable resource that can be used as a potential sustainable alternative to synthetic fibers, opening a new door for recycling of agricultural waste in sustainable cementitious materials.

**Acknowledgments** This work was financially supported by Fujian Ocean and Fishery Bureau (FJHJF-L-2022-19), Fuzhou Science and Technology Bureau (2021-P-031), Natural Science Foundation of China (51978171) and Minjiang Scholar program of Fujian province, China (GXRC-19045).

**Author contributions** Methodology, Conceptualization, Supervision, Writing- review & editing, Funding acquisition, Z.Y.; Investigation, Testing, Data analysis, Writing-original draft, K.Li.; and X.Yan., Investigation, Validation, Supervision, W.Wu.; Validation, Supervision, B.B.; and G.C.M. All authors reviewed the manuscript.

**Funding** This work was financially supported by Fujian Ocean and Fishery Bureau (FJHJF-L-2022–19), Fuzhou Science and Technology Bureau (2021-P-031), Natural Science Foundation of China (51978171) and Minjiang Scholar program of Fujian province, China (GXRC-19045).

**Data availability** The datasets used or analyzed during the current study are available from the corresponding author on reasonable request.

**Declarations**

**Ethical approval** The authors confirm that there were no ethical issues in preparing this manuscript.

**Consent for publication** All the authors listed have approved the manuscript for publication.

**Competing interests** The authors declare no competing interests.

## References

Alomayri T, Shaikh FUA, Low IM (2013) Characterisation of cotton fibre-reinforced geopolymer composites. Compos Part B Eng 50:1–6. https://doi.org/10.1016/j.compositesb.2013.01.013

Andiç-Çakir Ö, Sarikanat M, Tüfekçi HB, Demirci C, Erdoğan ÜH (2014) Physical and mechanical properties of randomly oriented coir fiber-cementitious composites. Compos Part B Eng 61:49–54. https://doi.org/10.1016/j.compositesb.2014.01.029

Bahja B, Elouafi A, Tizliouine A, Omari LH (2021) Morphological and structural analysis of treated sisal fibers and their im-pact on mechanical properties in cementitious composites. J Build Eng 34:102025. https://doi.org/10.1016/j.jobe.2020.102025

Boopathi L, Sampath PS, Mylsamy K (2012) Investigation of physical, chemical and mechanical properties of raw and alkali treated Borassus fruit fiber. Compos Part B Eng 43:3044–3052. https://doi.org/10.1016/j.compositesb.2012.05.002

Borchani KE, Carrot C, Jaziri M (2015) Untreated and alkali treated fibers from Alfa stem: effect of alkali treatment on structural, morphological and thermal features. Cellul 22(3):1577–1589. https://doi.org/10.1007/s10570-015-0583-5

do Amaral LM, de Souza Rodrigues C, Poggiali FSJ (2022) Hornification on vegetable fibers to improve fiber-cement composites: A critical review. J Build Eng 48:103947. https://doi.org/10.1016/j.jobe.2021.103947

Elzeadani M, Bompa DV, Elghazouli AY (2022) One part alkali activated materials: a state-of-the-art review. J Build Eng 57:104871. https://doi.org/10.1016/j.jobe.2022.104871

Guo B, Nakama S, Tian Q, Pahlevi ND, Hu Z, Sasaki K (2019) Suppression processes of anionic pollutants released from fly ash by various Ca additives. J Hazard Mater 371:474–483. https://doi.org/10.1016/j.jhazmat.2019.03.036

Huang Y, Tan J, Xuan X, Liu L, Xie M, Liu H, Zheng G (2021) Study on untreated and alkali treated rice straw reinforced geopolymer composites. Mater Chem Phys 262:124304. https://doi.org/10.1016/j.matchemphys.2021.124304

Huang Y, Tan J, Xuan X, Wei S, Liu L, Yu S, Zheng G (2022) Durability of plant fiber reinforced alkali activated composites. Constr Build Mater 314:125501. https://doi.org/10.1016/j.conbuildmat.2021.125501

Jiang D, An P, Cui S, Sun S, Zhang J, Tuo T (2020) Effect of modification methods of wheat straw fibers on water absorbency and mechanical properties of wheat straw fiber cement-based composites. Adv Mater Sci Eng 2020:1–14. https://doi.org/10.1155/2020/5031025

Jiang D, Shi C, Zhang Z (2022) Recent progress in understanding setting and hardening of alkali-activated slag (AAS) materials. Cem Concr Compos 134:104795. https://doi.org/10.1016/j.cemconcomp.2022.104795

Le Troëdec M, Sedan D, Peyratout C, Bonnet JP, Smith A, Guinebretiere R, Krausz P (2008) Influence of various chemical treatments on the composition and structure of hemp fibres. Compos A Appl Sci Manuf 39(3):514–522. https://doi.org/10.1016/j.compositesa.2007.12.001

Li K, Yang Z, Zhang Y, Li Y, Lu L, Niu D (2022) Effect of pretreated cow dung fiber on mechanical and shrinkage properties of cementitious composites. J Clean Prod 348:131374. https://doi.org/10.1016/j.jclepro.2022.131374

Li Q, Ibrahim L, Zhou W, Zhang M, Yuan Z (2021) Treatment methods for plant fibers for use as reinforcement in cement-based materials. Cellul 28:5257–5268. https://doi.org/10.1007/s10570-021-03903-w

Joffre T, Segerholm K, Persson C, Bardage SL, Hendriks CLL, Isaksson P (2017) Characterization of interfacial stress transfer ability in acetylation-treated wood fibre composites using X-ray microtomography. Ind Crops Prod 95:43–49. https://doi.org/10.1016/j.indcrop.2016.10.009

Juenger MCG, Winnefeld F, Provis JL, Ideker JH (2011) Advances in alternative cementitious binders. Cem Concr Res 41:1232–1243. https://doi.org/10.1016/j.cemconres.2010.11.012

Ma Y, Wu S, Zhuang J, Tong J, Qi H (2019) Tribological and physio-mechanical characterization of cow dung fibers reinforced friction composites: an effective utilization of cow dung waste. Tribol Int 131:200–211. https://doi.org/10.1016/j.triboint.2018.10.026

Mendes BC, Pedroti LG, Vieira CMF, Marvila M, Azevedo AR, de Carvalho JMF, Ribeiro JCL (2021) Application of eco-friendly alternative activators in alkali-activated materials: a review. J Build Eng 35:102010. https://doi.org/10.1016/j.jobe.2020.102010

Poletanovic B, Dragas J, Ignjatovic I, Komljenovic M, Merta I (2020) Physical and mechanical properties of hemp fibre reinforced alkali-activated fly ash and fly ash/slag mortars. Constr Build Mater 259:119677. https://doi.org/10.1016/j.conbuildmat.2020.119677

Reddy TRK, Rao TS, Suvarna RP (2013) Studies on thermal characteristics of cow dung powder filled glass-polyester hybrid composites. Compos Part B Eng 56:670–672. https://doi.org/10.1016/j.compositesb.2013.08.059

Santana HA, Júnior NSA, Ribeiro DV, Cilla MS, Dias CM (2021) Vegetable fibers behavior in geopolymers and alkali-activated cement based matrices: A review. J Build Eng 44:103291. https://doi.org/10.1016/j.jobe.2021.103291

Segal L, Creely JJ, Martin AE, Conrad CM (1959) An empirical method for estimating the degree of crystallinity of native cellulose using the X-ray diffractometer. Text Res J 29(10):786–794. https://doi.org/10.1177/004051755902901003

Sepe R, Bollino F, Boccarusso L, Caputo F (2018) Influence of chemical treatments on mechanical properties of hemp fiber reinforced composites. Compos Part B Eng 133:210–217. https://doi.org/10.1016/j.compositesb.2017.09.030

Sfez S, De Meester S, Dewulf J (2017) Co-digestion of rice straw and cow dung to supply cooking fuel and fertilizers in rural India: Impact on human health, resource flows and climate change. Sci Total Environ 609:1600–1615. https://doi.org/10.1016/j.scitotenv.2017.07.150

Shang X, Yang J, Song Q, Wang L (2020) Efficacy of modified rice straw fibre on properties of cementitious composites. J Clean Prod 276:124184. https://doi.org/10.1016/j.jclepro.2020.124184

Si R, Zhan Y, Zang Y, Sun Y, Huang Y (2023) Effect of basalt fiber on fracture properties and drying shrinkage of alkali-activated slag with different silicate modulus. J Mater Res Technol 25:552–569. https://doi.org/10.1016/j.jmrt.2023.05.211

Sun Y, de Lima LM, Rossi L, Jiao D, Li Z, Ye G, De Schutter G (2023) Interpretation of the early stiffening process in alkali-activated slag pastes. Cem Concr Res 167:107118. https://doi.org/10.1016/j.cemconres.2023.107118

Suwan T, Maichin P, Fan M, Jitsangiam P, Tangchirapat W, Chindaprasirt P (2022) Influence of alkalinity on self-treatment process of natural fiber and properties of its geopolymeric composites. Constr Build Mater 316:125817. https://doi.org/10.1016/j.conbuildmat.2021.125817

Tang Z, Yang X, Jiang H, Cong X, Tian W, Lu S (2023) Biomodification of bond performance of coconut fiber in cement mortar to enhance damping behavior. J Mater Civil Eng 35:04023351. https://doi.org/10.1061/jmcee7.mteng-15933

Toledo Filho RD, Ghavami K, Sanjuán MA, England GL (2005) Free, restrained and drying shrinkage of cement mortar composites reinforced with vegetable fibres. Cem Concr Compos 27:537–546. https://doi.org/10.1016/j.cemconcomp.2004.09.005

Tong Y, Zhao S, Ma J, Wang L, Zhang Y, Gao Y, Xie Y (2014) Improving cracking and drying shrinkage properties of cement mortar by adding chemically treated luffa fibres. Constr Build Mater 71:327–333. https://doi.org/10.1016/j.conbuildmat.2014.08.077

Van Nguyen C, Mangat PS (2020) Properties of rice straw reinforced alkali activated cementitious composites. Constr Build Mater 261:120536. https://doi.org/10.1016/j.conbuildmat.2020.120536

Vinod A, Gowda TGY, Vijay R, Sanjay MR, Gupta MK, Jamil M, Siengchin S (2021) Novel Muntingia Calabura bark fiber reinforced green-epoxy composite: a sustainable and green material for cleaner production. J Clean Prod 294:126337. https://doi.org/10.1016/j.jclepro.2021.126337

Wei J, Meyer C (2015) Degradation mechanisms of natural fiber in the matrix of cement composites. Cem Concr Res 73:1–16. https://doi.org/10.1016/j.cemconres.2015.02.019

Wongsa A, Kunthawatwong R, Naenudon S, Sata V, Chindaprasirt P (2020) Natural fiber reinforced high calcium fly ash geopolymer mortar. Constr Build Mater 241:118143. https://doi.org/10.1016/j.conbuildmat.2020.118143

Yang X, Li L, Zhao W, Tian Y, Zheng R, Deng S, Mu Y (2023) The influence of potassium hydroxide concentration and temperature on pulp characteristics and cow dung-based paper performance. J Nat Fibers 20:2164546. https://doi.org/10.1080/15440478.2022.2164546

Yurt Ü (2020) An experimental study on fracture energy of alkali activated slag composites incorporated different fibers. J Build Eng 32:101519. https://doi.org/10.1016/j.jobe.2020.101519

Yusefi M, Khalid M, Yasin FM, Abdullah LC, Ketabchi MR, Walvekar R (2018) Performance of cow dung reinforced bio-degradable poly (Lactic Acid) biocomposites for structural applications. J Polym Environ 26:474–486. https://doi.org/10.1007/s10924-017-0963-z

Zhang B, Zhu H, Cheng Y, Huseien GF, Shah KW (2022) Shrinkage mechanisms and shrinkage-mitigating strategies of alkali-activated slag composites: a critical review. Constr Build Mater 318:125993. https://doi.org/10.1016/j.conbuildmat.2021.125993

Zhang J, Shi C, Zhang Z, Ou Z (2017) Durability of alkali-activated materials in aggressive environments: a review on recent studies. Constr Build Mater 152:598–613. https://doi.org/10.1016/j.conbuildmat.2017.07.027

Zhou B, Wang L, Ma G, Zhao X, Zhao X (2020) Preparation and properties of bio-geopolymer composites with waste cotton stalk materials. J Clean Prod 245:118842. https://doi.org/10.1016/j.jclepro.2019.118842

Zhou X, Zeng Y, Chen P, Jiao Z, Zheng W (2021) Mechanical properties of basalt and polypropylene fibre-reinforced alkali-activated slag concrete. Const Build Mater 269:121284. https://doi.org/10.1016/j.conbuildmat.2020.121284

Zhang L, Sun X (2017) Using cow dung and spent coffee grounds to enhance the two-stage co-composting of green waste. Bioresour Technol 245:152–161. https://doi.org/10.1016/j.biortech.2017.08.147